Chapter 5

Day Ahead Scheduling of PHEV in Presence of Local DER Modules

5.1 Introduction

The last chapter addressed the 24-hour coordinated scheduling of DGs. The scheduling has been investigated by simulating different penetration levels of PHEVs along with different demand response (DR) levels. This chapter presents a day ahead scheduling of PHEVs in presence of Local DER modules. In this chapter, scheduling of PHEVs charging/discharging is obtained between arrival time and departure time of vehicles.

In the current scenario, DERs have become an important part of the power system structure. In the near future, integration of DGs and BESS into the distribution system can be utilized to support the grid when the distribution system experience significant loads of electric vehicles. In recent years, BESS and V2G operation mode of electric vehicle has been proposed to manage the residential loads at higher scale. Utilization of EV with DER units can be used to support the residential load demand by dynamic adjustment of EVs charging/discharging profile. Hence, the proper scheduling of PHEVs (between start trip time and last trip arrival time), Distributed- Battery Energy Storage System (D-BESS) and DGs are required to ensure reliable service of distribution system.

In this chapter, a 24-hour day-ahead scheduling of PHEVs (between start trip time and last trip arrival time), DGs and D-BESSs to optimize four objectives (i.e. cost, CO_2 emission, real power losses and load flattening) have been proposed simultaneously by keeping the consumer loads intact. The weighted sum method is used to deal with the proposed multi-objective function and a new optimization technique, Effective Butterfly Optimizer (EBO), is used to solve the optimization problem in this chapter. In addition to this, a possible way to tune the weights of objective function is to quantify the effect of each objective function with respect to listed objectives on the distribution system planning and operation is also investigated in this chapter.

5.2 Problem Formulation

In this section, mathematical model of utility operating cost of (CPG, DG, BESS and PHEV), CO_2 emission, losses and load flattening in the distribution network are formulated. Four objective functions are considered in this study which include CPG, DGs, D-BESS and PHEVs (G2V/V2G mode). The time step is taken one hour in throughout the problem formulation and any changes in power consumed/produced by PHEVs, DGs and D-BESSs behavior with in hour is neglected.

5.2.1 Objective function

The proposed optimization model aims to minimized objective function (F) which consists cost of energy (f_1), CO_2 emission (f_2), losses (f_3) and load flattening (f_4). Main objective function (F) which is expressed as follows.

$$Min.F\{(f_1, f_2, f_3, f_4)\}.$$

The cost of energy (f_1) is calculated as the sum of (i) cost of CPG's energy (F_{CPG}), (ii) cost of DGs power (F_{DGs}), (iii) curtailment cost of DGs (F_{GCP}), (iv) cost of discharging of PHEVs (F_{PHEV}) and (V) cost of discharging of D-BESS (F_{D-BESS}). It is to be noted that charging cost of PHEVs and D-BESS is already included in F_{CPG}. Thus, the cost of energy can be expressed as follows.

$$f_1 = F_{CPG} + F_{DGs} + F_{GCP} + F_{PHEV} + F_{D-BESS}, \tag{5.1}$$

where,

$$F_{CPG} = \sum_{h=1}^{24} E_{CPG}(h)C_c(h) \times 1Hour,$$

$$F_{DG} = \sum_{d=1}^{N_{DG}} \sum_{h=1}^{24} E_{DG}(d,h) C_{DG}(d,h) \times 1Hour,$$

$$F_{GCP} = \sum_{d=1}^{N_{DG}} \sum_{h=1}^{24} E_{GCP}(d,h) C_{GCP}(d,h) \times 1Hour,$$

$$F_{PHEV} = \sum_{e=1}^{N_{PHEV}} \sum_{h=1}^{24} [E_{Discharge}^{PHEV}(e,h) C_d(h)] \times 1Hour,$$

$$F_{D-BESSs} = \sum_{b=1}^{N_{D-BESS}} \sum_{h=1}^{24} [E_{Discharge}^{D-BESS}(b,h) C_d(h)] \times 1Hour.$$

The necessary modification in objective function of existing literature is given in Appendix IV.

The CO_2 emission (f_2) is calculated as the sum of CO_2 emission due to energy generation of CPG (E_{CO_2-CPG}), fuel cell (FC) DGs and shaving off CO_2 due to PHEVs.

$$f_2 = E_{CO_2-CPG} + E_{CO_2-DG} - E_{CO_2-PHEV}. \tag{5.2}$$

Where,

$$E_{CO_2-CPG} = \sum_{h=1}^{24} E_{CPG}(h) K_{CO_2-CPG} \times 1000,$$

$$E_{CO_2-DG} = \sum_{d=1}^{N_{DG}} \sum_{h=1}^{24} E_{DG}(d,h) K_{CO_2-DG} \times 1000,$$

$$E_{CO_2-PHEV} = \sum_{e=1}^{N_{PHEV}} \sum_{h=1}^{24} D_{km} K_{CO_2-PHEV} \times 1000.$$

The energy losses (f_3) is calculated as the sum of total energy loss in the system.

$$f_3 = \sum_{h=1}^{24} \sum_{m \in s^i} \sum_{i=1}^{N_B} 0.5 r_{ik} \frac{|V_B(i,h)| - |V_B(k,h)|}{|z_{ik}|^2}, \tag{5.3}$$

where,

$m \in s^i$ is set of all the buses that have been directly connected to i^{th} bus.

For the load flattening (f_4), a flat load curve is desirable for the system which is formulated as follows.

$$f_4 = \sum_{h=1}^{24} (t_d(h) - \overline{t_d})^2, \tag{5.4}$$

where,

Table 5.1: Variation in weighing factor

Weight	Set-A	Set-B	Set-C	Set-D
w_1	0.45	0.25	0.15	0.15
w_2	0.25	0.45	0.25	0.25
w_3	0.15	0.15	0.45	0.15
w_4	0.15	0.15	0.15	0.45

$t_d(h)$ and $\overline{t_d}$ are total demand and average demand at Point of Common Coupling (PCC) at h^{th} hour, which is supplied by CPG.

$$t_d(h) = \sum_{i=1}^{N_B}\Bigg(P_{load}(i,h) + \sum_{b=1}^{N_{D-BESS}} (E^{D-BESS}_{Charge}(i,h,b) - E^{D-BESS}_{Discharge}(i,h,b)) + \sum_{e=1}^{N_{PHEV}} (E^{PHEV}_{Charge}(i,h,e) - E^{PHEV}_{Discharge}(i,h,e))\Bigg) + \sum_{i=1}^{N_{Branch}} E_{loss}(i,h) - \sum_{d=1}^{N_{DG}} E_{DG}(h,d).$$

$\overline{t_d}$ is average power demand during 24 hours and can be defined as,

$$\overline{t_d} = \frac{1}{24}\sum_{h=1}^{24} t_d(h).$$

The multi-objective function (F) is formulated as the weighted sum approach of f_1, f_2, f_3 and f_4 which is shown as follows.

$$F = min\{(f_1, f_2, f_3, f_4)\} = w_1 f_1^2 + w_2 f_2^2 + w_3 f_3^2 + w_4 f_4^2. \tag{5.5}$$

Where, w_1, w_2, w_3 and w_4 are user supplies weights which corresponds to relative importance of one's prefer objective function. Each sets of weights generate one optimal solution at a time. However in this work, there are four set of weights as listed in Table. 5.1, are considered to quantify the relative effects of objective function with respect to each other. For example, in set-A, when the cost of energy (f_1) is treated as 45% relative importance, whereas CO_2 emission, energy losses and load flattening based objective function get weights of 25%, 15% and 15% respectively. The problem is to determine the optimal values of $E_{DG}(d,h)$, $E^{PHEV}_{Charge}(e,h)$, $E^{PHEV}_{Discharge}(e,h)$, $E^{D-BESS}_{Charge}(b,h)$, $E^{D-BESS}_{Disharge}(b,h)$ for a given pattern of $C_{DG}(d,h)$, $C_c(h)$, $C_d(h)$ and $t_d(h)$.

5.2.2 Constraints

Several constraints including power flow constraint, bus voltage magnitude, maximum and minimum DGs power limit, limit on number of DGs, CPG maximum limit and battery technical limit for PHEV and D-BESS are considered for the optimization problem formulation in this research. The details of the constraints are as follows.

Energy balance constraints

$$\sum_{h=1}^{24} P_{loss}(h) = \sum_{d=1}^{N_{DG}}\sum_{h=1}^{24} E_{DGs}(d,h) + \sum_{h=1}^{24} E_{CPG}(h) + \sum_{e=1}^{N_{PHEV}}\sum_{h=1}^{24} E_{Discharge}^{PHEV}(e,h) - \sum_{i=1}^{N_B}\sum_{h=1}^{24} P_{load}(i,h)$$
$$- \sum_{e=1}^{N_{PHEV}}\sum_{h=1}^{24} E_{Charge}^{PHEV}(e,h) - \sum_{b=1}^{N_{D-BESS}} E_{Charge}^{D-BESS}(b,h) + \sum_{b=1}^{N_{D-BESS}} E_{Discharge}^{D-BESS}(b,h), \tag{5.6}$$

where,

$$P_{loss}(h) = \sum_{k\in s^i}\sum_{i=1}^{N_B} 0.5\frac{r_{ik}|V_B(i,h) - V_B(k,h)|^2}{|z_{ik}|^2}.$$

$$\sum_{h=1}^{24} Q_{loss}(h) = \sum_{h=1}^{24} Q_{CPG}(h) - \sum_{i=1}^{N_B}\sum_{h=1}^{24} Q_{load}(i,h), \tag{5.7}$$

where,

$$Q_{loss}(h) = \sum_{k\in s^i}\sum_{i=1}^{N_B} 0.5\frac{x_{ik}|V_B(i,h) - V_B(k,h)|^2}{|z_{ik}|^2}.$$

It is assumed that PHEVs and DGs does not consume or produce reactive power from/to the distribution system.

Equation (5.6) & (5.7) represents active and reactive power balance on the distribution system. These equation ensure the generation and load demand on distribution system should be matched all times.

Bus voltage magnitude

$$V_i^{min} \le V_B(i,h) \le V_i^{max}. \tag{5.8}$$

Constraint (5.8) ensure that the bus voltages are within the specified limit.

Maximum and minimum DG Limit

$$E_{DG}(d,h) \le X_{DG}(d,h) \times E_{DG-max}(d,h), \tag{5.9}$$

$$E_{DG}(d,h) \ge X_{DG}(d,h) \times E_{DG-min}(d,h), \tag{5.10}$$

where,

$X_{DG}(d,h)$ is the binary number (0,1), which represents the connection status of DGs on candidate bus. So, that if $X_{DG}(d,h) = 0$ which means the there is no exchange of power, whereas if $X_{DG}(d,h) = 1$ which means there is exchange of power.

DGs maximum and minimum power range is restricted in constraints (5.9) & (5.10).

PHEVs and D-BESS technical constraints at i^{th} bus

Constraints related to limits of PHEV's battery and D-BESS are given by equations (5.11) - (5.21).

$$E^{PHEV}_{Charge}(e,i) \times E^{PHEV}_{Discharge}(e,i) = 0, \tag{5.11}$$

$$E^{D-BESS}_{Charge}(b,i) \times E^{D-BESS}_{Discharge}(b,i) = 0. \tag{5.12}$$

Constraints (5.11) & (5.12) ensures that the charging and discharging of PHEV's battery and D-BESS will not take place simultaneously at i^{th} bus.

$$E^{PHEV}_{store}(e,h) = E^{PHEV}_{store}(e,h-1) + E^{PHEV}_{Charge}(e,h) - E^{PHEV}_{Used}(e,h) - E^{PHEV}_{Discharge}(e,h), \tag{5.13}$$

$$E^{D-BESS}_{store}(b,h) = E^{D-BESS}_{store}(b,h-1) + E^{D-BESS}_{Charge}(b,h) - E^{D-BESS}_{Used}(b,h) - E^{D-BESS}_{Discharge}(b,h). \tag{5.14}$$

Constraints (5.13) & (5.14) shows the energy balance equation for PHEV battery and D-BESS.

$$E^{PHEV}_{Discharge}(e,h) \times \frac{1}{\eta_d} \leq E^{PHEV}_{store}(e,h-1), \tag{5.15}$$

$$E^{PHEV}_{Charge}(e,h) \times \eta_c \leq BC_{PHEV}(e) - E^{PHEV}_{store}(e,h-1). \tag{5.16}$$

$$E^{D-BESS}_{Discharge}(b,h) \times \frac{1}{\eta_d} \leq E^{D-BESS}_{store}(b,h-1), \tag{5.17}$$

$$E^{D-BESS}_{Charge}(b,h) \times \eta_c \leq BC_{D-BESS} - E^{D-BESS}_{store}(b,h-1). \tag{5.18}$$

Constraints (5.15) - (5.18) restricted the battery charging and discharging limit considering battery balance for PHEVs and D-BESS.

$$SOC^{PHEV}_{min}(e) \leq SOC^{PHEV}(e,h) \leq SOC^{PHEV}_{max}(e), \tag{5.19}$$

$$SOC^{D-BESS}_{min}(b) \leq SOC^{D-BESS}(b,h) \leq, SOC^{D-BESS}_{max}(b), \tag{5.20}$$

where, $SOC^{PHEV}_{min}(e)$, $SOC^{D-BESS}_{min}(b)$ are minimum possible limit for PHEVs and D-BESSs. Whereas, $SOC^{PHEV}_{min}(e)$, $SOC^{D-BESS}_{min}(b)$ are possible maximum limit for PHEVs and D-BESSs.

Constraints (5.19) & (5.20) ensure that the SOC of PHEVs and D-BESSs at h^{th} hour restricted within the capacity limit.

$$SOC_{t_{dep}}(e) = \left[min\left(100, \left(SOC_{t_{arr}}(e) + \frac{E_{g2v,max}(e)}{BC_{PHEV}(e)} \times \Delta T \times 100 \right) \right) \right], \tag{5.21}$$

where,

$$\Delta T = \begin{cases} (t_{dep} - t_{arr}) & t_{arr} < t_{dep} \\ 24 + (t_{dep} - t_{arr}) & t_{arr} > t_{dep}. \end{cases}$$

Constraints to get maximum possible SOC of e^{th} PHEVs at departure time are imposed in (5.21).

5.3 Problem Solving Methodology

5.3.1 Power flow analysis

The modified Current Injection Newton-Raphson based load flow Method (MCINR) is used to perform power flow analysis. To validate efficacy and robustness of proposed load flow algorithm $MCINR$ is tested on both the unbalanced radial system (18-, 84- and 140-bus) and meshed distribution test systems (24-, 118- and 300-bus) in chapter-3. It is observed that the convergence characteristic in terms of maximum power mismatch is better in case of modified current injection Newton-Raphson ($MCINR$) as compared to existing current injection based load flow algorithm. In this method $2n$ set of current injection equation are written in rectangular coordinates and the jacobian matrix ($2n \times 2n$) has the same structure as nodal admittance matrix [158]. The program for $MCINR$ power flow was coded in MATLAB.

5.3.2 Optimization methodology

Butterfly Optimizer (BO) is a population based global optimization technique based on the mate locating behavior of male butterflies [165]. This algorithm is efficient and easy to implement, compared with other bio-inspired algorithms. But, it may sometime converge to a local optimum solution in hard problems. To address this issue, Abhishek at al., add a Binomial mutation to EBO to improve the global convergence [166]. This global improved algorithm called Effective Butterfly Optimizer (EBO). As a consequence, in practice, it might be hard to validate the performance derived by EBO. In an attempt to address the validation of performance, a variant of EBO, EBOwithCMAR outperformed all the state-of-the-algorithms bench mark problems of $CEC - 2017$ [166].

EBO is a dual population based algorithm, where two different populations are initialized within the search space of problem. In every iteration individual in a populations update themselves by using patrolling or perching strategies of the algorithm in such a way to reach the optimum solution. Main procedure of EBO is shown in the form of flowchart in Fig. 5.1. The process of EBO is divided into five steps: initialization, condition-I, perching, patrolling, condition-II.

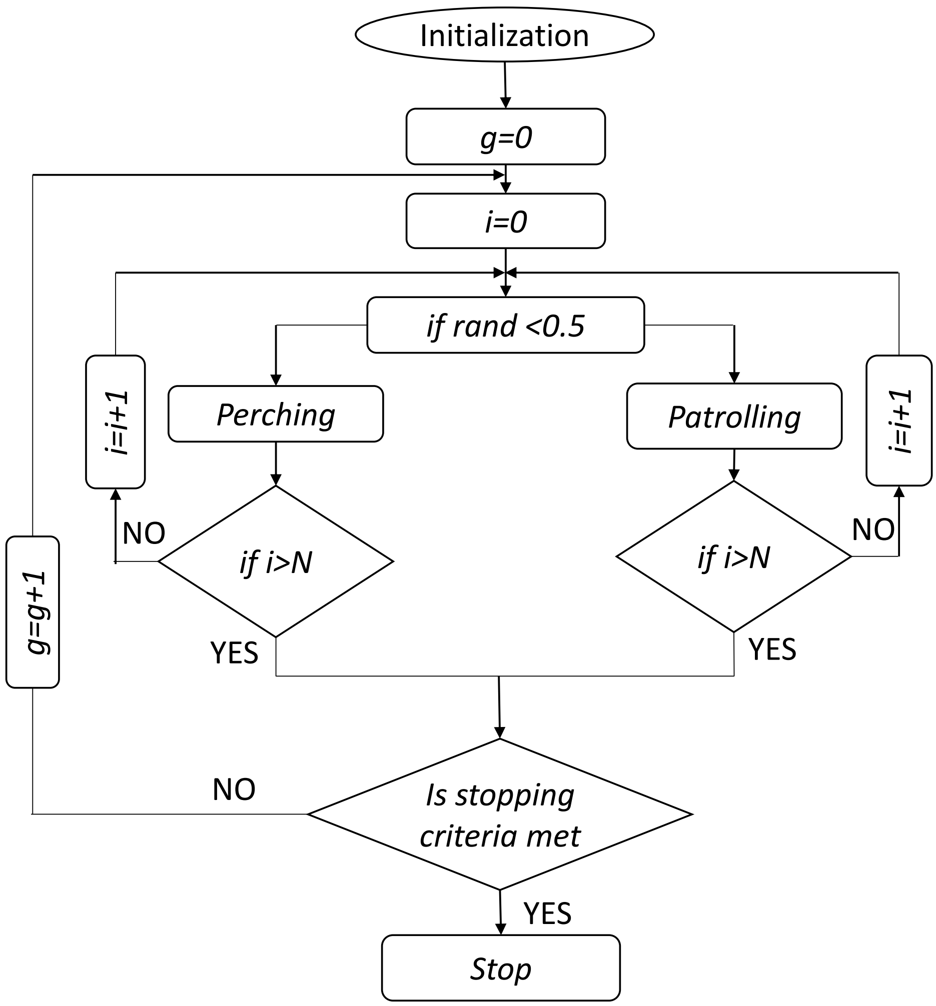

Figure 5.1: Flow chart diagram of Effective Butterfly Optimizer (EBO)

Initialization

In the initialization process the population and all the required parameters are initialized. The initialized population covers the entire search space through uniformly distributed numbers. These random variables are within the prescribed lower and upper boundary limits for each of the variable.

$$\vec{ss}_{min} = \{ss_{1min}, ss_{1min}, ..., ss_{Dmin}\}, \tag{5.22}$$

$$\vec{ss}_{max} = \{ss_{1max}, ss_{1max}, ..., ss_{Dmax}\}. \tag{5.23}$$

The initial location of the j^{th} index of the i^{th} individual of population-I, can be generated as follows.

$$\dot{x}_{ij} = ss_{j,min} + rand[0,1].(ss_{j,max} - ss_{j,min}), \tag{5.24}$$

where, $rand[0,1]$ is a uniformly distributed random number within the range $[0,1]$.

Similarly, the initial value of the j^{th} index of the i^{th} individual of population-II is generated as follows.

$$\dot{mx}_{ij} = ss_{j,min} + rand[0,1].(ss_{j,max} - ss_{j,min}). \tag{5.25}$$

Initial velocity vector of i^{th} individual is calculated using equation (5.26).

$$\vec{\dot{v}_i} = \vec{\dot{x}_i} - \vec{m}\dot{x}_i. \tag{5.26}$$

After initialization, all the individuals proceed for iteration until the condition-II is satisfied. Two variable criss cross and attractive neighbors of all individuals are re initialized at the beginning of every iteration before entering the main process of EBO. Criss cross and most attractive neighbors variable are used in perching and patrolling strategy respectively. The crisscross vector $\vec{cc}^k$ is generated as follows.

$$\vec{cc}^k = randperm[1,n] = \{cc_1^k, cc_2^k, ..., cc_N^k\}, \tag{5.27}$$

where, $randperm[1,N]$ is a random permutation of number between 1 and N.

In original BO [165], the most attractive neighbors of all individual is same and the individuals having lower fitness value are selected as most attractive neighbors. In every iteration, EBO employs the perching or patrolling operation to update the positions of individual in both populations. Condition-I is a criteria which selects the update strategy of individual out of the two updating methods namely perching and patrolling. Condition-II is applied as the termination criteria for the optimization process of EBO.

Condition-I

In original BO [165], the success history of every individuals is used to select the updating strategies. The previous success or failure of updating strategy of each individual is applied as condition-I. If the individual updates its location in population-I, then that individual will go with same updating-strategy for next iteration. If the individual does not update its location in population-I then the updating-strategy for next iteration will be different.

Perching

Perching is the strategy to update the population after the iteration in EBO. Initially all the individuals prefer the perching updating-strategy to update the location of individual on search space in population-I and population-II. The process of perching is shown in Fig. 5.2. The update strategy is divided into three sub-operators: criss-cross modification, crossover and selection which are as follows.

Criss-cross modification

EBO generates a criss-cross modification vector, $\vec{u}_i^k$ for i^{th} individual, which is selected for the perching updating-strategy. Criss-cross modification vector, $\vec{u}_i^k$ is calculated by using equation 5.28.

$$\vec{u}_i^k = R\{\vec{x}_{ui}^k, \vec{mx}_{ui}^k\} + F\left(R\{\vec{x}_{pi}^k, \vec{mx}_{pi}^k\} - R\{\vec{x}_{qi}^k, \vec{mx}_{qi}^k\}\right), \tag{5.28}$$

where, $R\{a, b\}$ is a random selection operator in which probability of selection of a and b is equal to 0.5. p_i and q_i are integer valued variable, which are generated according to equation (5.29).

$$p_i \neq q_i \neq u_i \neq i. \tag{5.29}$$

Crossover

After criss-cross modification, the modified criss cross vectors ($\vec{u}_i^k$) do crossover with the target individual ($\vec{x}_i^k$) to generate $\vec{y}_i^k$. In original BO, one point crossover is applied to generate the $\vec{y}_i^k$. In one point crossover, only one index of criss-cross modified vector $\vec{u}_i^k$ takes place in $\vec{y}_i^k$ and remaining elements of $\vec{y}_i^k$ is equal to $\vec{x}_i^k$. The crossover index is generated randomly within range $[1, D]$. The one-point crossover is employed by EBO as

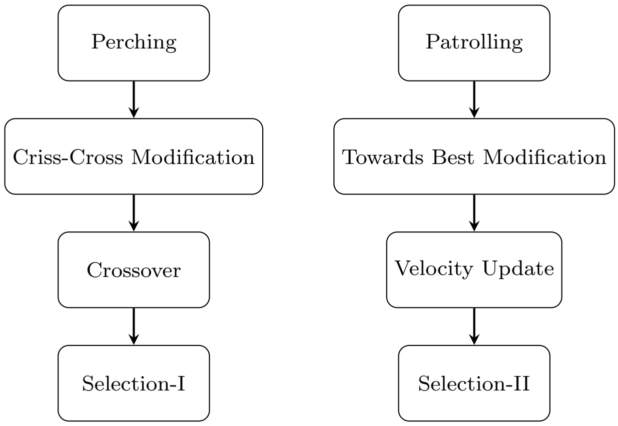

Figure 5.2: Process of patrolling and perching

follows.

$$\vec{y}_i^{(k+1)} = \begin{cases} y_{ij}^k & if j == m \\ x_{ij}^k & otherwise \end{cases} \tag{5.30}$$

where, m is an integer randomly chosen between 1 and D.

Selection-I

Selection compares the vector $\vec{y}_i^{(k+1)}$ with vector $\vec{x}_i^k$ in terms of their fitness value to update the location of i^{th} individual in population-I to the next iteration.

$$\vec{x}_i^{(k+1)} = \begin{cases} \vec{y}_i^{(k+1)} & if \left(\vec{y}_i^{(k+1)}\right) \leq f\left(\vec{x}_i^k\right) \\ \vec{x}_i^k & otherwise. \end{cases} \tag{5.31}$$

Patrolling

In EBO, patrolling is one of the strategy to update the population towards the most attractive individual. Process of patrolling is shown in Fig. 5.2. Patrolling is also divided into three sub-operators: towards best modification, velocity update and selection-II which are described as follows.

Towards best modification

EBO generates the towards best modified vector $\vec{w}_i^k$ for each target vector $\vec{x}_i G$ using,

$$\vec{w}_i^{(k+1)} = \vec{x}_i^k + F\left(\vec{V}_i^k + \vec{x}_{maxuv}^k - \vec{x}_i^k\right), \tag{5.32}$$

where, $maxuv$ is the most attractive neighbour of the target individual i.

Velocity update

After towards the best modification, velocity vector of target individual i is updated using,

$$\vec{v}_i^{(k+1)} = \begin{cases} \vec{w}_i^{(k+1)} - \vec{x}_i^k & f\left(\vec{w}_i^{(k+1)}\right) \leq f\left(\vec{x}_i^k\right) \\ F\left(\vec{v}_i^k + \vec{x}_{maxuv}^k - \vec{x}_i^k\right) & otherwise. \end{cases} \tag{5.33}$$

Selection-II

It compares the location of the target individual i in population-I, $\vec{x}_i^k$ towards the best modified vector $\vec{w}_i^k$ to update the location of target individual i in population-I for the next iteration.

$$\vec{x}_i^{(k+1)} = \begin{cases} \vec{w}_i^{(k+1)} & f\left(\vec{w}_i^{(k+1)}\right) \leq f\left(\vec{x}_i^k\right) \\ \vec{x}_i^k & otherwise \end{cases} \tag{5.34}$$

5.4 System Model

The 38-bus distribution system network [163] shown in Fig. 3.2 has been considered for this study. The detailed specification with bus-wise load type and MVA capacity of the test system can be found in [163]. The system data and types of customers are listed in Appendix I. The distribution system is energized through CPG which is connected at bus-1. For this 38-bus system of ref. [163], hourly average load distribution of ref. [2] has been considered. A total of 160 PHEVs and 160 BESS are considered in this study. Following assumptions are made in this study.

- PHEVs and D-BESSs are equally scattered on residential buses.
- Charging/discharging of PHEVs and D-BESS are done only at residential buses.
- All the residential buses are well equipped with the V2G and G2V facility for charging/discharging of PHEVs and DGs from/to the distribution system.

The tariff related to electricity price and the cost paid by DSO to customer for discharging the PHEVs battery and D-BESS into the grid are given in Table 4.1. The rate of charging and discharging of PHEVs and D-BESS is taken as 4 kW/hr, 1.6 kW/hr for PHEV battery and BESS respectively whereas, discharging rate is 2.8 kW/hr and 0.8 kW/hr for EV battery and BESS respectively. The battery capacity of D-BESS is considered as

4 kWh. The charging and discharging efficiency are taken as 95% for both the PHEVs and D-BESS. In this study, for the above-mentioned 38-bus system, selection of candidate buses for the DGs integration are determined on the basis of minimization of energy losses in the system. These locations will be the input to the system model. The selection of candidate buses has been performed for all dispatchable DGs in 38-bus system using a Mixed Integer Non-Linear Programming (MINLP) approach as given in Appendix III .

In this study, for the above mentioned test system, candidate buses for curtailable DGs installation are determined on the basis of minimization of energy losses in the system. These locations will be the input to the system model. The detailed characteristics of DGs including the type of DGs and the hourly availability are given in Appendix II as reported in [164]. The selection of candidate buses has been performed for all dispatchable DGs in 38-bus system using a Mixed Integer Non-Linear Programming (MINLP) approach as given in Appendix III. The penetration of DGs is not constant throughout the problem, it is varied according to the suitability of DSO. The maximum number of DGs can be installed is taken ten, which can be scheduled in steps to optimize the problem. The curtailment cost of DGs are considered as 40% of the individual DGs cost. The CO_2 emission related parameters used in this study is given in Table 5.2 [15]. The tariff related to electricity price and the cost paid by DSO to customer for discharging the PHEVs battery into the grid are given in Table 4.1.

Table 5.2: CO_2 emission related parameters

$K_{CO_2-CPG}(kg/kWh)$	$K_{CO_2-DG}(kg/kWh)$	$K_{CO_2-PHEV}(kg/km)$
143	307	0.338

5.5 Case Studies: Results and Discussions

To determine the effectiveness of the objective function formulated in this study, a 24 hour scheduling is performed. The PHEVs are scheduled in such a way that the consumers will get maximum possible level of SOC at departure time at a reduced cost. The D-BESSs are scheduled such that all D-BESSs are maintained at SOC level greater than 30% for emergency purpose i.e power cut.

The charging and discharging of PHEVs and D-BESS can have both beneficial and adverse effects on the distribution system. The uncertainty in loading pattern due to increased penetration of PHEVs and introduction of D-BESS affects the distribution system parameters such as peak load, voltage profile, energy losses and energy cost. The scheduled charging and discharging of PHEVs and D-BESS during peak loads can be used for saving off the peaks (V2G). The DGs present in the distribution system will have their own effects. It is important to study the effects of DGs in the distribution system with PHEV penetration and D-BESS. It is also important to segregate the effects of unscheduled PHEVs charging, scheduled charging/discharging of PHEVs and D-BESS, and effects of DGs so that one may be able to understand their individual and combined effects.

Following three case studies are designed to demonstrated the effects PHEVs, D-BESS and DGs.

1. Case-I (Base case): This case considers unscheduled charging i.e, vehicle will be charged just after the last trip arrival of PHEVs is assumed. This case will serve as base case to compare the effects of inclusion of scheduled PHEVs and D-BESS charging/discharging with and without DGs. In this case following system characteristics are studies are performed.

    (a) Loading pattern and peak load for residential load.
    (b) Hourly voltage profile and bus-wise voltage profile.
    (c) Energy losses.
    (d) Overall energy cost.

2. Case-II (System with scheduled PHEVs and D-BESS charging/discharging): In this case it is assumed that all the scheduled charging/discharging of PHEVs and D-BESS are equally scattered at residential buses. In this case following study is performed.

    (a) Comparison of loading pattern for case-I and case-II.
    (b) Hourly voltage profile and bus-wise voltage profile in presence of scheduled PHEVs and D-BESS with unscheduled PHEVs charging.
    (c) Comparison of energy losses with case-I (base case).

(d) Comparison of energy cost with the base case when PHEVs and D-BESS are scheduled.

3. Case-III (System with scheduled PHEVs and D-BESS with DGs): In this case effect of addition of DGs to the system with PHEVs and D-BESS are demonstrated. The following system characteristics are studied.

   (a) Effect of DGs on loading pattern and peak load of the system.

   (b) Effect of addition of DGs on hourly voltage profile and bus-wise voltage profile.

   (c) Effect of addition of DGs on system energy losses and comparison of energy losses.

   (d) Effect on the system energy cost.

All sequential steps of the proposed methodology are exhibited in Fig. 5.3 and calculation process of each parameter for all cases are as follows.

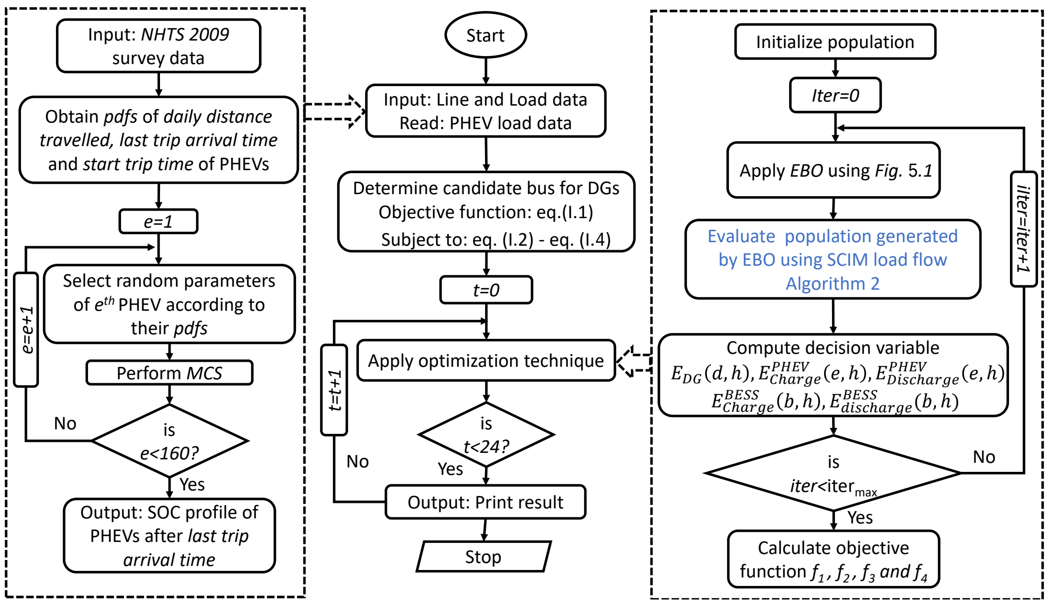

Figure 5.3: Flow chart of proposed method

- Perform simulation of proposed approach according to flow chart as shown in Fig. 5.3.

- Get values of f_1, f_2, f_3 and f_4 as output from Fig.5.3.

- Compute multi-objective function (F) as the weighted sum approach of f_1, f_2, f_3 and f_4 which is shown as,

$$F = min\{(f_1, f_2, f_3, f_4)\} = w_1 f_1^2 + w_2 f_2^2 + w_3 f_3^2 + w_4 f_4^2.$$

- Compute Peak-to-Average Ratio (PAR) as;

$$PAR = \frac{Max[t_d(h)]}{\overline{t_d}}.$$

- Get value of V_{min} as

$$V_{min.} = Min[V_B(i,h)]$$

- Compute utility cost (U.C) as;

$$U.C = \sum_{h=1}^{24} \Bigg(\sum_{i=1}^{N_B} P_{Load}(i,h) + \sum_{d=1}^{N_{DG}} \sum_{h=1}^{24} E_{DG}(d,h) C_{DG}(d,h) - E_{GCP}(d,h) C_{GCP}(d,h)$$
$$+ \sum_{e=1}^{N_{PHEV}} E_{Discharge}^{PHEV}(e,h) C_d(h) + \sum_{b=1}^{N_{D-BESS}} E_{Discharge}^{D-BESS}(b,h) C_d(h) + \sum_{i=1}^{N_{Branch}}$$
$$E_{loss}(i,h) - \sum_{e=1}^{N_{PHEV}} E_{Charge}^{PHEV}(e,h) + \sum_{b=1}^{N_{D-BESS}} E_{Charge}^{D-BESS}(b,h) \Bigg)$$

- Compute residential consumer cost (C.C) as;

$$C.C = \sum_{h=1}^{24} \Bigg(\Bigg(\sum_{i \forall R} P_{Load}(i,h) + \sum_{e=1}^{N_{PHEV}} E_{Charge}^{PHEV}(i,e,h) + \sum_{b=1}^{N_{D-BESS}} E_{Charge}^{D-BESS}(i,b,h) \Bigg)$$
$$C_c(h) - \Bigg(\sum_{e=1}^{N_{PHEV}} E_{Discharge}^{PHEV}(i,e,h) + \sum_{b=1}^{N_{D-BESS}} E_{Discharge}^{D-BESS}(i,b,h) \Bigg) \Bigg),$$

where, $R \epsilon \{2, 5, 12, 14, 19, 22, 31, 32\}$.

5.5.1 Case-I: (Base case)

The base case represents the system with unscheduled PHEVs charging. Unscheduled charging of PHEVs means that the charging is started just after the last trip arrival time and it will continue until the battery becomes fully charged. This base case study is just for reference which will reflect the worst situation that the consumers are independent of maintaining distribution system performance.

The overall loading pattern and peak load demand are shown in Fig. 5.4. Unscheduled PHEV charging, bus-wise voltage of the system, hourly minimum voltage of the

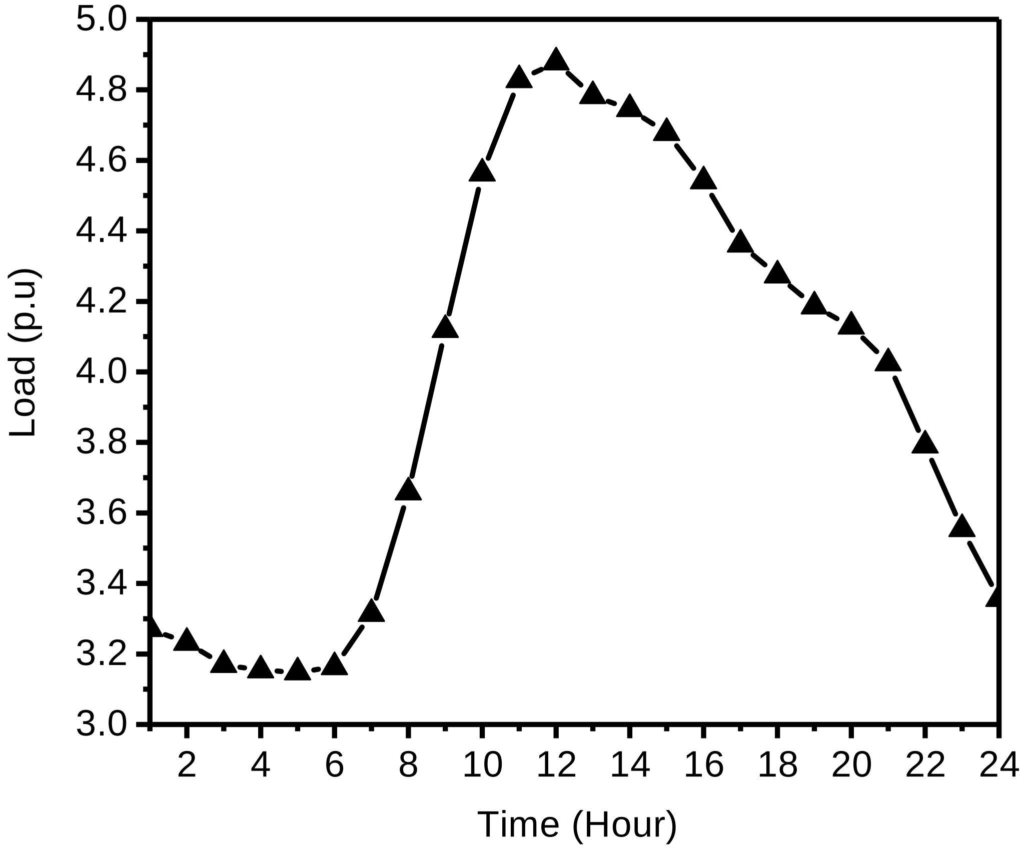

Figure 5.4: Case:I Overall load demand

system and hourly energy loss of the system are shown in Figs. 5.5, 5.6, 5.7 and 5.8 respectively. Following are the observations.

- Fig. 5.4: Peak load demand occurs at 12 : 00 hour and valley hour at 04 : 00 hour.
- Fig. 5.5: PHEVs charging takes place through out the day which is just after the last trip arrival time. This scenario is independent of the loading scenario of the system.
- Fig. 5.6: Bus-wise voltage for peak hour (12 : 00 hour) is lower than valley hour (04 : 00 hour).
- Fig. 5.7: Voltage deviation from slack bus is more during peak hour (12 : 00 hour).
- Fig. 5.8: Losses are higher during peak hours. Basically, the energy losses of the system reflect the overall load demand of the system. i.e. during peak hours energy losses are more as compared to the valley hours.

The outcomes of the base case is depicted in Table 5.3.

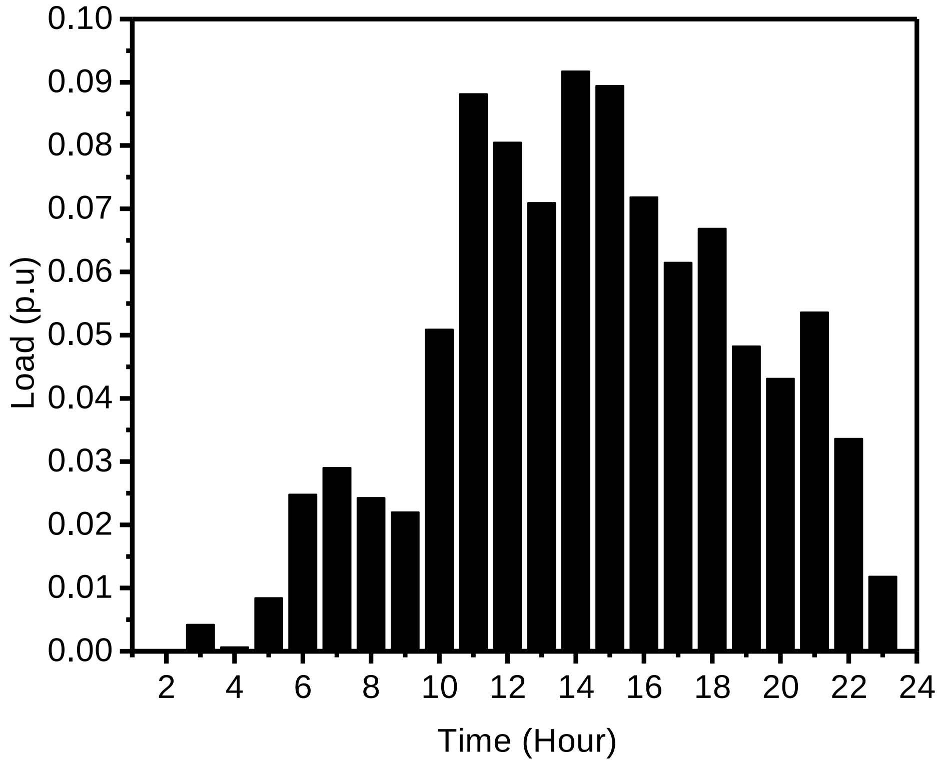

Figure 5.5: Case:I Unscheduled PHEV power

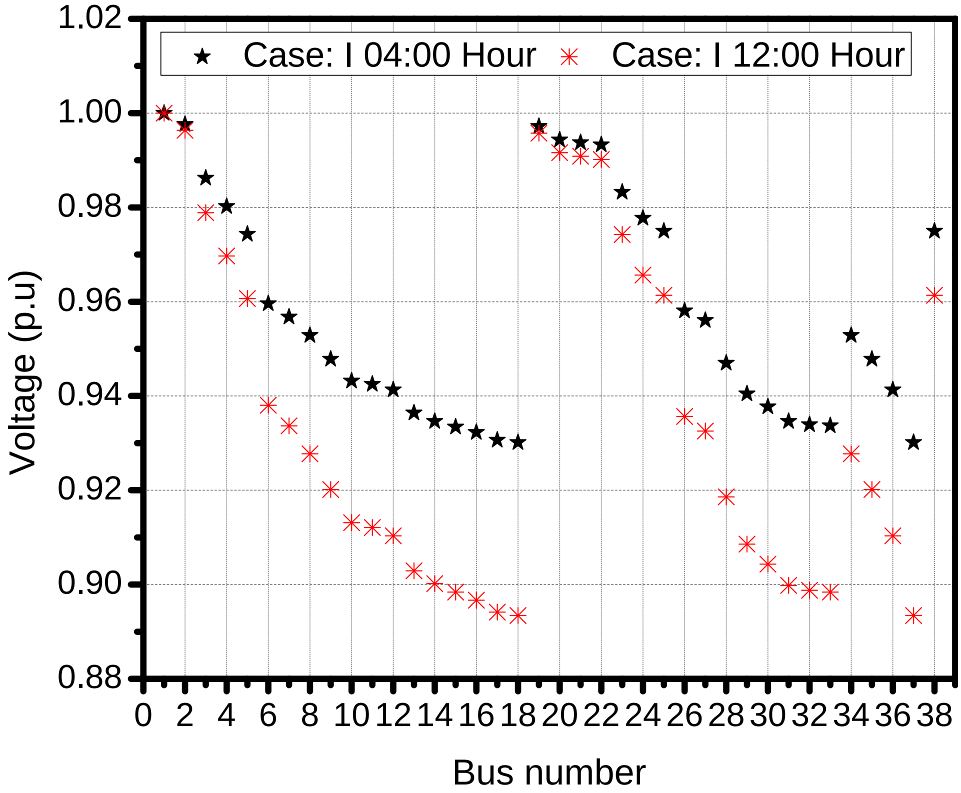

Figure 5.6: Case:I Voltage profile during peak hours (12^{th} Hour) and valley hours (04^{th} hour)

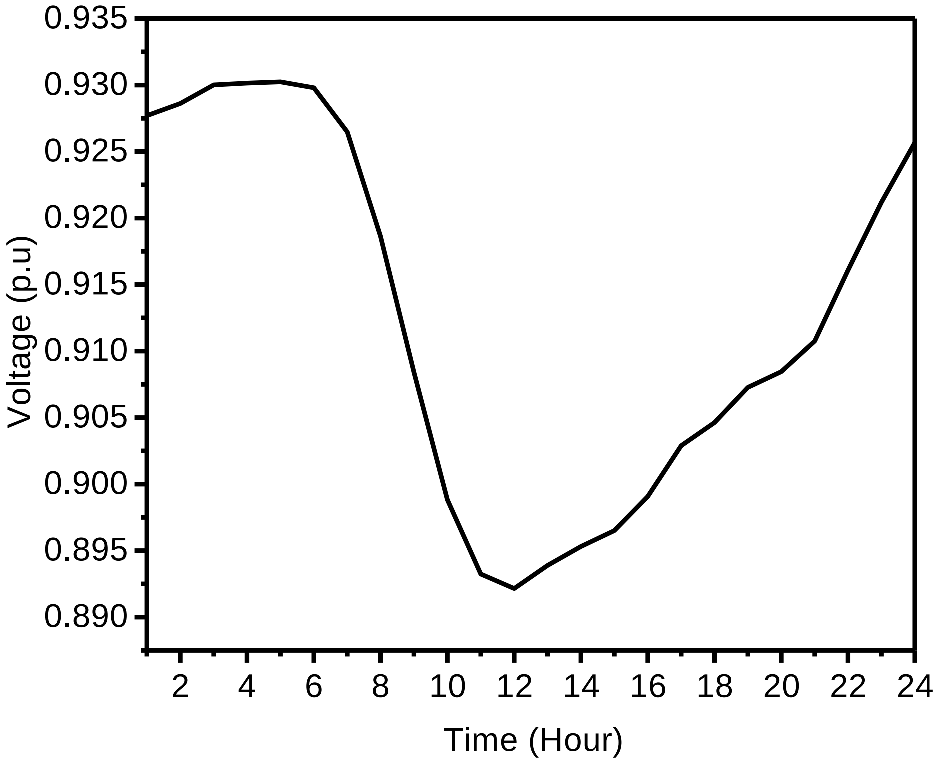

Figure 5.7: Case:I Hourly minimum voltage

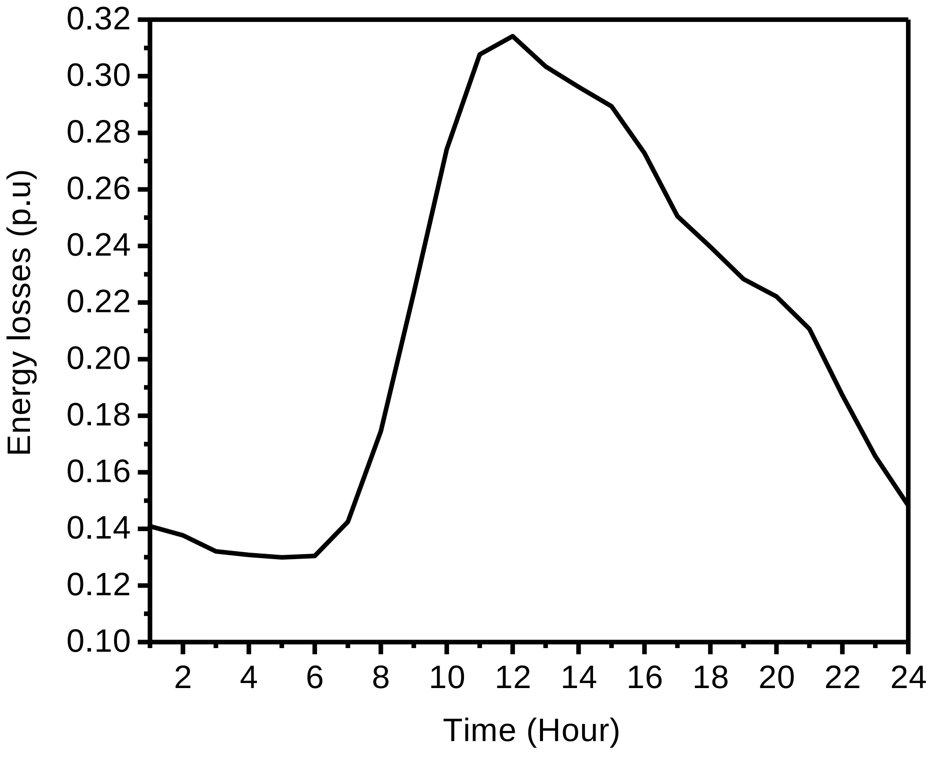

Figure 5.8: Hourly energy loss

Table 5.3: Outcomes of base case

Cost(f_1)(€)	CO_2 emission(kg/kWh) (f_2)	Loss (f_3)(MW)	Load flattening (f_4) (p.u)	
9692.5	1.34336×10^5	5.0527	9.115	
F	PAR	V_{min}(p.u)	Utility cost	Consumer cost
1	1.2334	0.8921	96.92.5	2305.1

5.5.2 Case-II: System with scheduled PHEVs and D-BESS

In this case, the PHEVs and D-BESS charging/discharging are scheduled in between the *last-trip-arrival-time* of vehicle and *start-trip-time* of vehicle. The D-BESS charging/discharging is also scheduled for a day. This case basically shows how the distribution system performance is improved, if the charging/discharging of PHEVs and D-BESS is scheduled in advance.

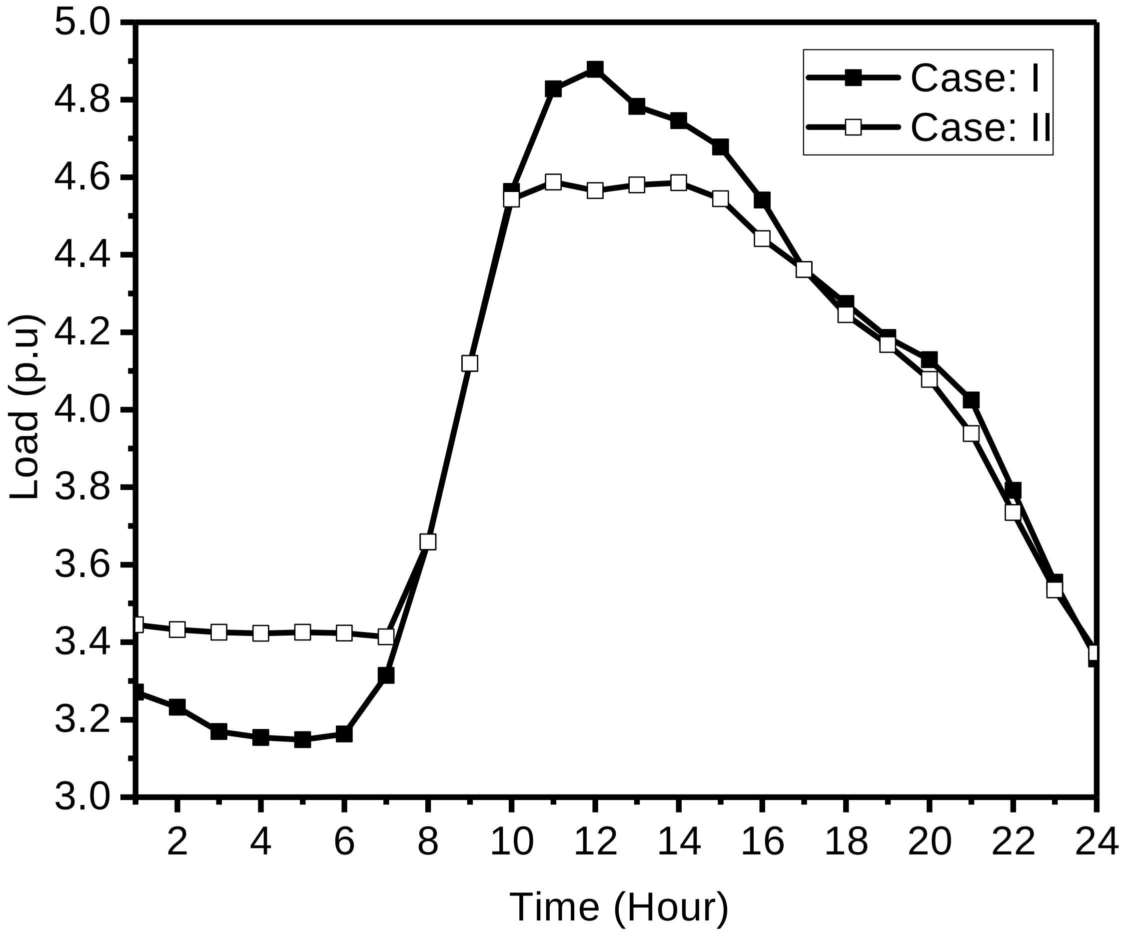

Figure 5.9: Case:II Comparison of overall loading pattern

Comparison of load profile between case-I and case-II, hourly PHEVs power scheduling in between *last-trip-arrival-time* and *start-trip-time*, hourly D-BESS power scheduling, comparison of hourly energy losses for case-I and case-II, comparison of hourly minimum voltage, comparison of bus-wise voltage for case-I and case-II are shown in Figs. 5.9, 5.10, 5.11, 5.12, 5.13 and 5.14 respectively. Following are the observations.

- Fig. 5.9: If PHEVs and D-BESS charging are properly scheduled then the overall load profile improves and the Peak-to-Average Ratio (PAR) of the system is improved by 0.0788 p.u for case-I.

- Fig. 5.10: Most of the PHEVs charging will take place in peak hours and most of the vehicle discharging will takes place in valley hours (positive part of bar chart: PHEVs charging power, negative part of bar chart: discharging of PHEVs power, solid line: total net power due to PHEVs in the distribution system).

- Fig. 5.11: Almost all the D-BESS charging will take place in valley hours and it will discharge to supply power to the distribution system during the peak hours.

- Fig. 5.12: During 01 : 00 - 07 : 00 hour energy loss reduces and in the period of 11 : 00 - 16 : 00 hour energy losses increases. However, in totality energy losses are reduced by 0.0288 MW.

- Fig. 5.13: At peak hour (12 : 00 hour) bus wise voltage of the system is improved.

- Fig. 5.14: Minimum voltage is improved by 0.0051 unit at 12 : 00 hour (peak hour) in comparison to case-I.

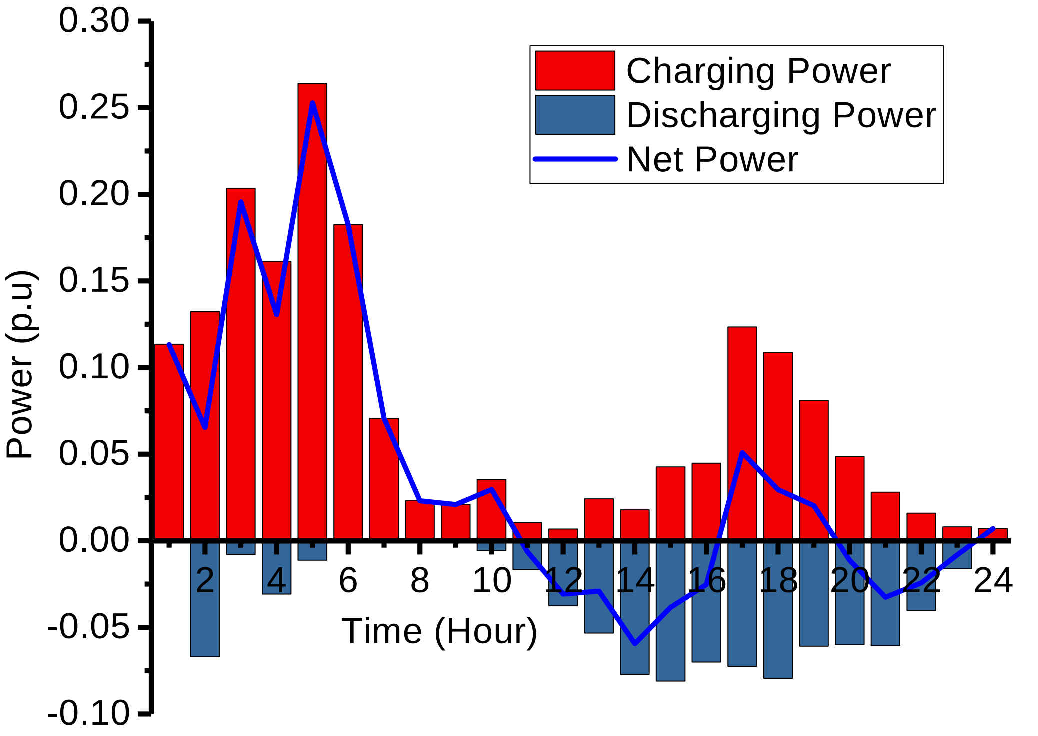

Figure 5.10: Case:II Hourly PHEV power scheduling

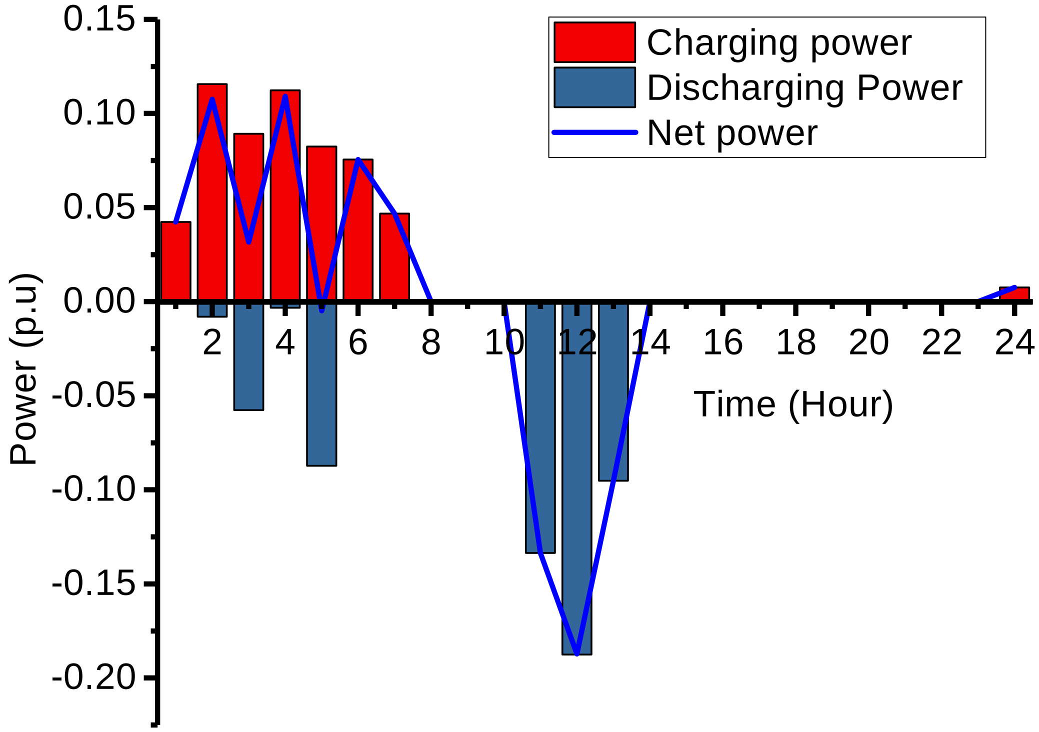

Figure 5.11: Case:II Hourly BESS power scheduling

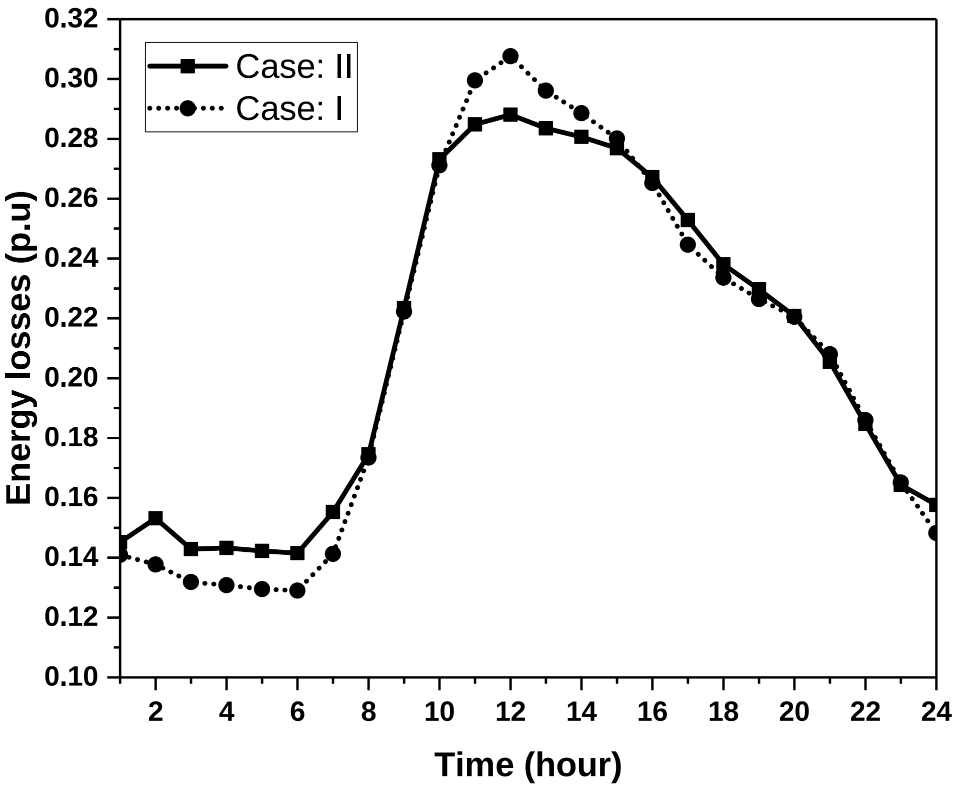

Figure 5.12: Case:II Hourly energy losses

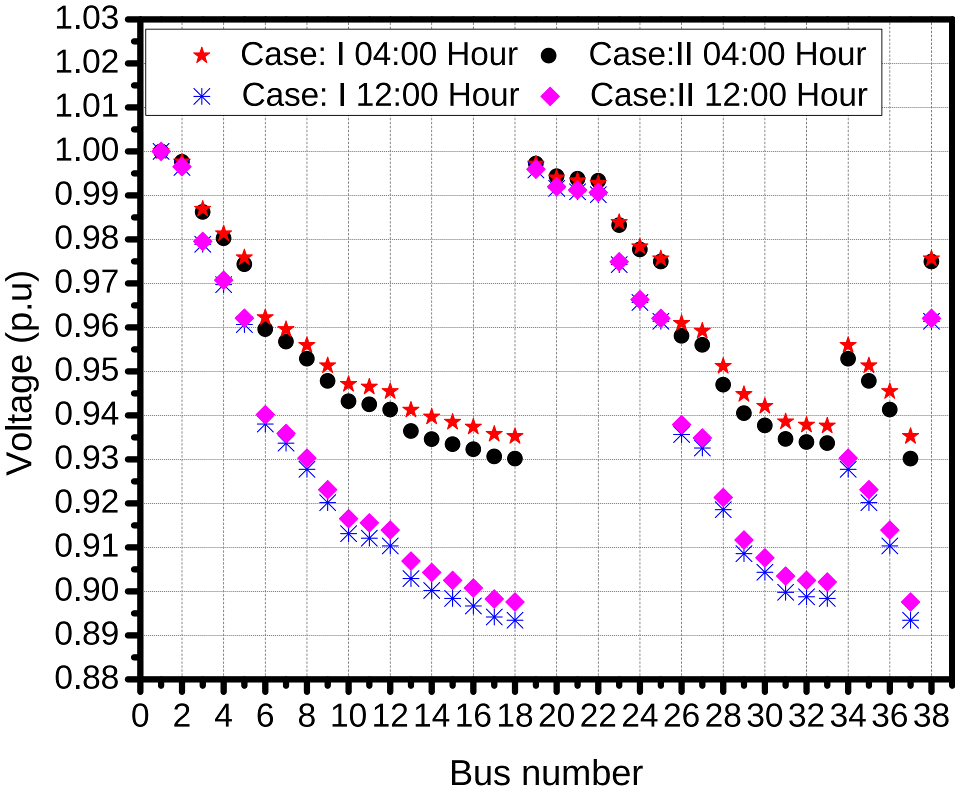

Figure 5.13: Case:II Bus wise voltage

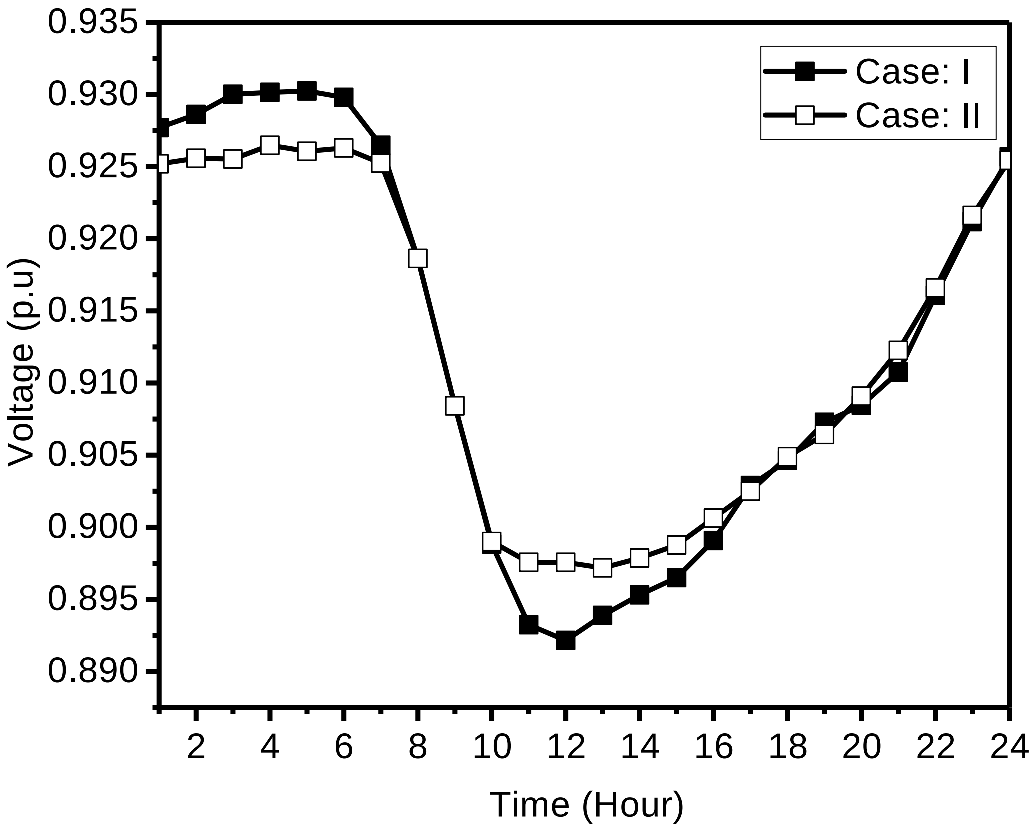

Figure 5.14: Case:II Hourly minimum voltage

The outcome of case-II is summarized in Table 5.4. As the summary of case-II, it is observed that if PHEVs and D-BESS charging/discharging are scheduled in optimized manner then the overall distribution system performance gets improved as well as cost related to utility and residential consumer is decreases. Additional study with varying weight of objective function is also performed for case-II. The outcome with the varying weight of objective function is presented in Table 5.5. It is observed that, if cost of energy (f_1) is treated as higher weight, then overall system cost as well as consumer cost is lower as compare to with consideration of other set of weights. whereas, if load flattening based objective function (f_4) is treated as higher weightage, then with little sacrifice of cost, value of f_4 is significantly reduced.

Table 5.4: Outcomes of Case-II

Cost(f_1)(€)	CO_2 emission(kg/kWh) (f_2)	Loss (f_3)(MW)	Load flattening (f_4) (p.u)	
9760.0	1.34467×10^5	5.0239	5.36	
F	PAR	V_{min}(p.u)	Utility cost (€)	Consumer cost (€)
0.95	1.1548	0.8975	9588.4	2243.3

Table 5.5: Case-II Variation of weightage of objective function

Weightage	[0.45,0.25,0.15,0.15]	[0.25,0.45,0.15,0.15]	[0.15,0.25,0.45,0.15]	[0.15,0.25,0.15,0.45]
Cost(f_1)(€)	9767.0	9778.2	9793.1	9811.4
$Co_2emission(kg/kWh)(f_2)$	1.34467×10^5	1.34486×10^5	1.34521×10^5	1.34558×10^5
Loss (f_3)(MW)	5.0239	5.0242	5.0254	5.0281
Load flattening (f_4) (p.u)	5.36	5.333	5.308	0.958
F	0.95	0.949	0.946	0.835
PAR	1.1548	1.1543	1.1532	1.1505
V_{min}(p.u)	0.8975	0.8974	0.8973	0.8975
Utility Cost (€)	9588.4	9588.0	9586.2	9589.5
Consumer cost (€)	2243.3	2246.4	2250.8	2255.5

5.5.3 Case-III: (System with scheduled PHEVs and D-BESS with DGs)

In this case, coordinated scheduling of PHEVs, D-BESS and DGs are studied. The optimal locations of distributed generations are determined based on reduced line losses and operating cost. The distributed generations consist of PV, WT and fuel cell.

Comparison of load curve between cases-I, II and III, PHEVs power scheduling for case-III, D-BESS power scheduling for case-III, hourly DGs power scheduling for case-III, comparison of energy losses between cases-I, II and III, and comparison of hourly minimum voltage between cases-I, II and III are shown in Figs. 5.15, 5.16, 5.17, 5.18, 5.19 and 5.20 respectively. Following are the observations.

- Fig. 5.15: PHEVs charging/discharging are synchronized according to load curve. i.e during the valley hours charging will take place and during peak hours PHEVs discharging will take place.

- Fig. 5.16: D-BESS charging/discharging are synchronized according to load curve. i.e during the valley hours charging will take place and during peak hours D-BESS discharging will take place.

- Fig. 5.17: All DGs optimal power are shown by separate line curve. It can be observed that most of DG power is scheduled during the peak load hour as opposed to the valley hour.

- Fig. 5.18: Load curves in case-III are significantly improved after coordinated scheduling of PHEVs, D-BESS and DGs. It is observed that the demand on the main substation gets lowered when DGs are employed into the system and scheduled along with PHEVs and D-BESSs. The PAR of the system in case-III is equal to 1.0045 due to synchronized charging/discharging of PHEVs and D-BESS.

- Fig. 5.19: This figure shows comparison of energy losses for Case-I, Case-II and Case-III. It is observed that the in Case-II energy loss is slightly lower as compare to Case-II (Base Case) and overall total energy loss gets significantly reduced to 3.292 MW when system is incorporated with DGs.

- Fig. 5.20: It is also observed that after coordinated scheduling of PHEVs, D-BESS and DGs, the voltage profile of the system improves significantly. As far as system hourly voltage profile is concerned in Case-I and Case-II, it is observed that there is small improvement in voltage profile during valley hour for Case-II but in Case-III it is significantly improved.

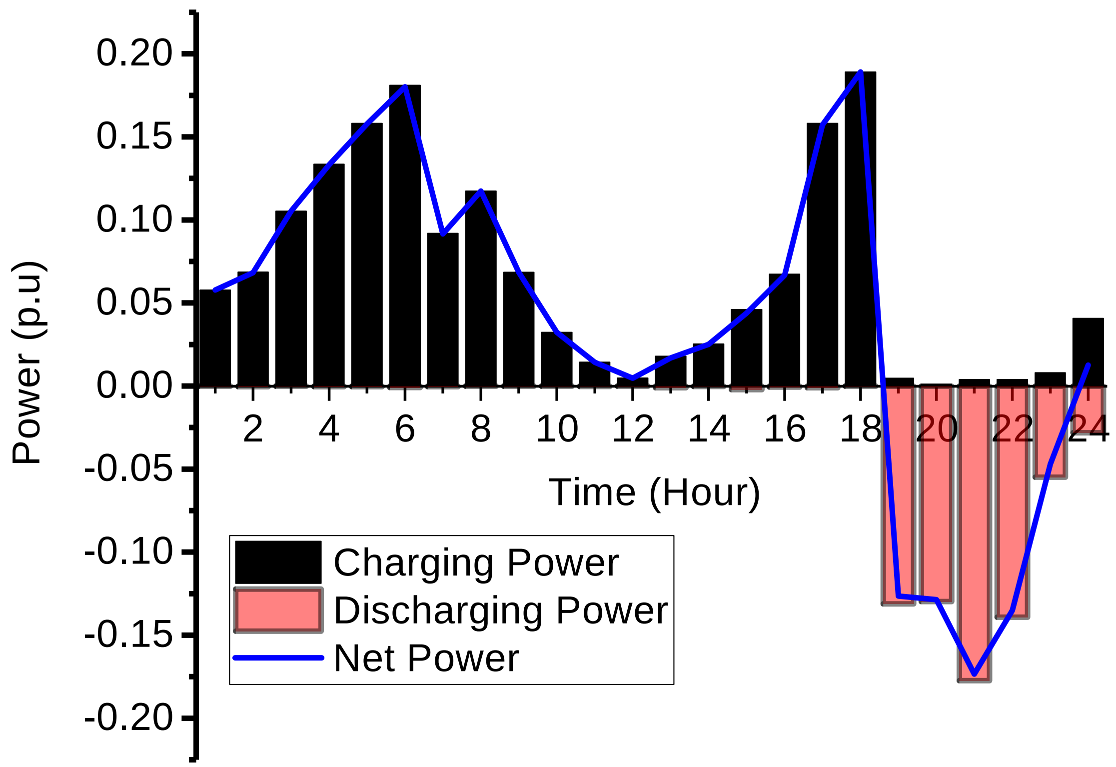

Figure 5.15: Case:III Hourly PHEV power scheduling

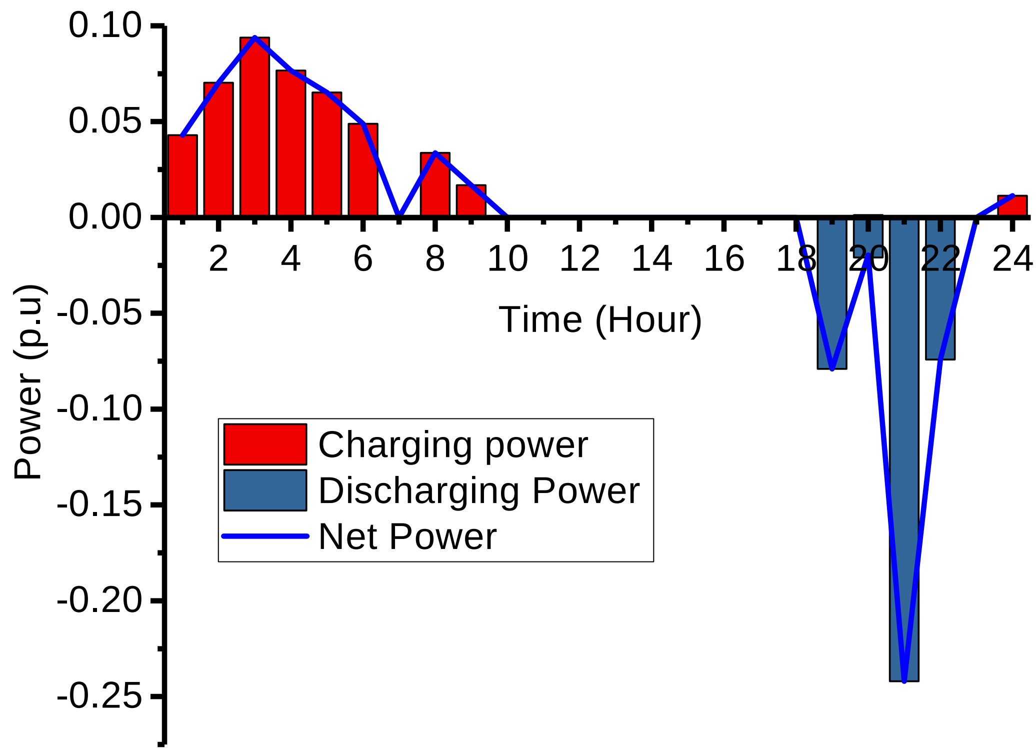

Figure 5.16: Case:III Hourly BESS power scheduling

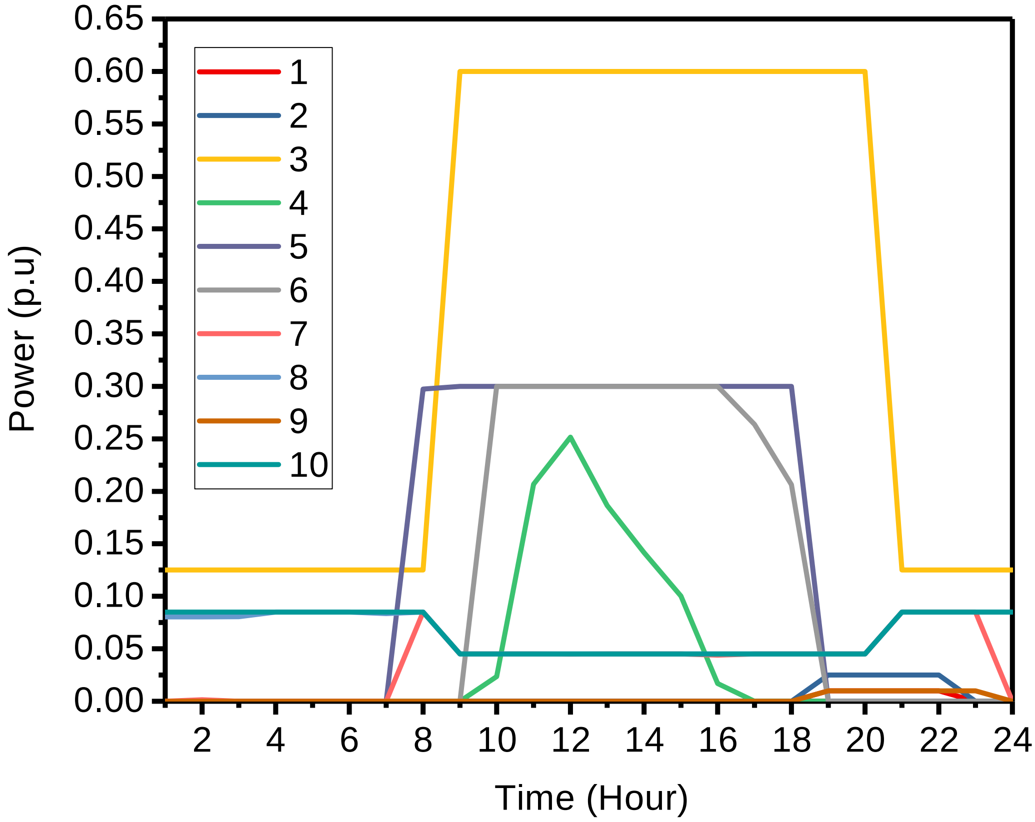

Figure 5.17: Case:III Hourly DG power scheduling

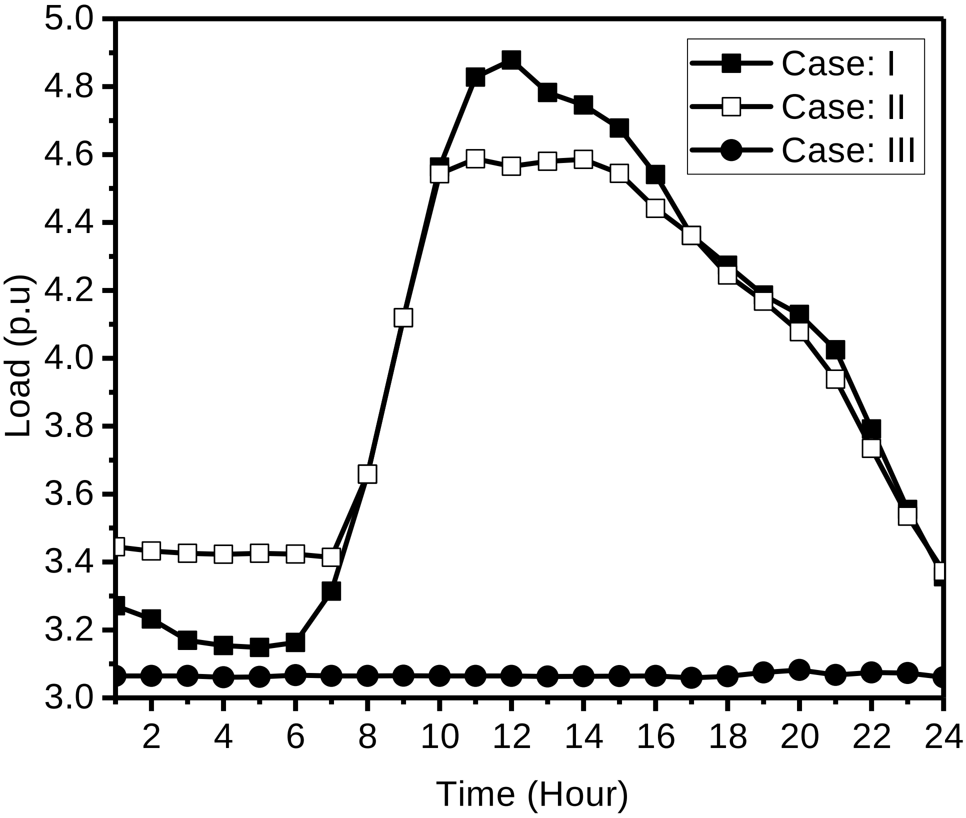

Figure 5.18: Case:III Flatten load

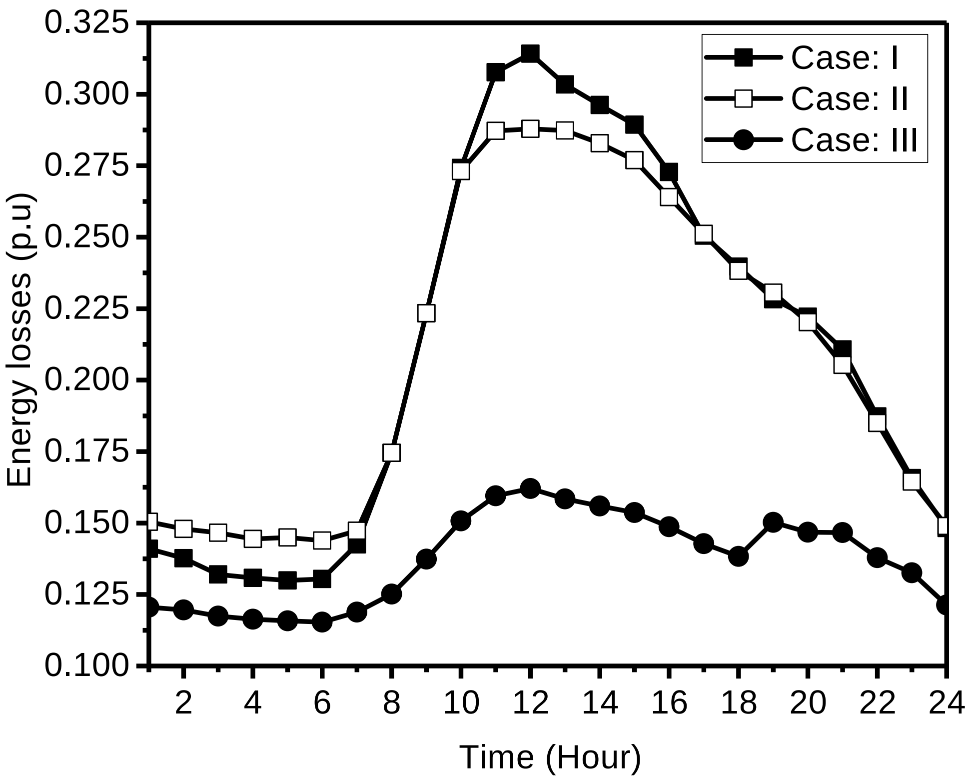

Figure 5.19: Case:III Hourly energy losses

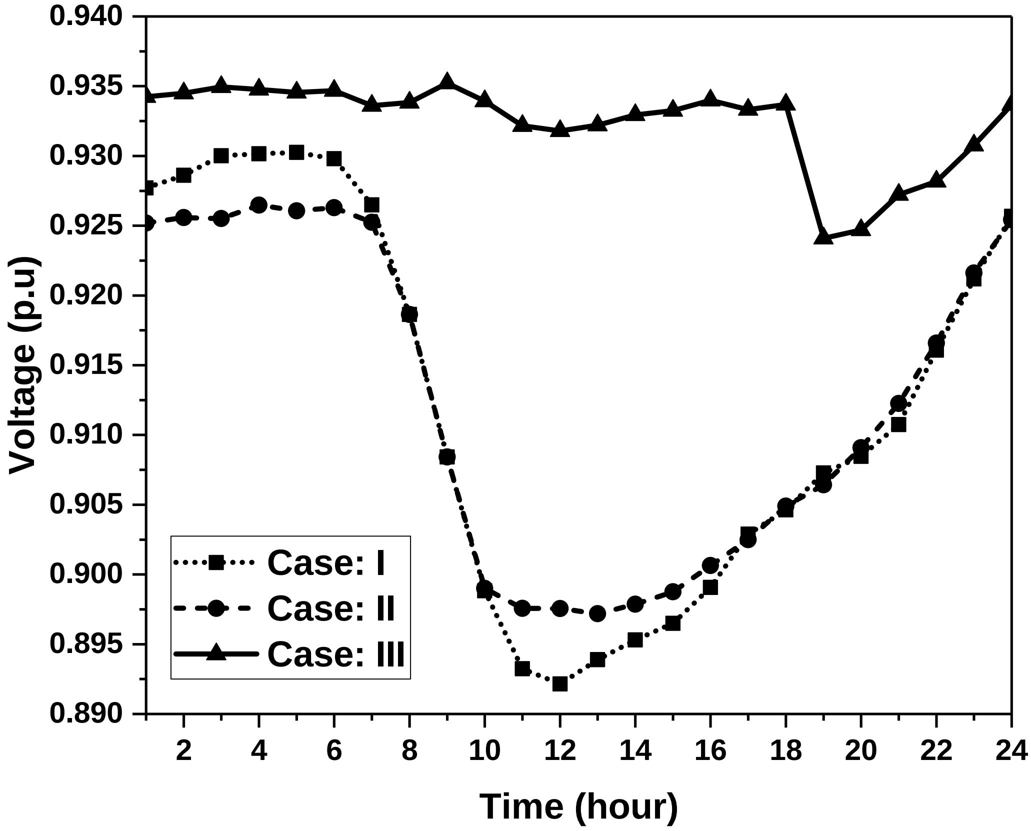

Figure 5.20: Case:III Hourly minimum voltage

The outcomes of Case-III is summarized in Table 5.6. It is observed that, after optimal scheduling of the DGs with scheduled charging/discharging of PHEVs and D-BESS, the cost to utility increases from 9588.4 to 10194.0 €/day and cost to residential consumers decreases from 2243.3 to 2212.1 €/day. As a summary, the proposed idea increases the cost of utility but benefits the consumers charging/discharging into the distribution system. Additional study with varying weight of objective function is also performed for Case-III. The outcome with the varying weight of objective function is presented in Table 5.7. The SOC level of PHEVs at departure is shown in Fig. 5.21. it is observed that most of the vehicles have enough SOC level to meet daily driving distance.

Table 5.6: Outcomes of Case-III

Cost(f_1)(€)	Co_2 emission(kg/kWh) (f_2)	Loss (f_3)(MW)	Load flattening (f_4) (p.u)	
10194.0	1.0439×10^5	3.2941	0.00067	
F	PAR	V_{min}(p.u)	Utility cost (€)	Consumer cost (€)
0.896	1.0045	0.9242	10019.8	2212.1

Table 5.7: Case-III Variation of weightage for objective function

Weightage	[0.45,0.25,0.15,0.15]	[0.25,0.45,0.15,0.15]	[0.15,0.25,0.45,0.15]	[0.15,0.25,0.15,0.45]
Cost(f_1)(€)	10194.0	10208.6	10282.5	10232.9
$Co_2emission(kg/kWh)(f_2)$	1.0439×10^5	1.0443×10^5	1.04353×10^5	1.04406×10^5
Loss $(f_3)(MW)$	3.2941	3.2846	3.2646	3.2770
Load flattening (f_4) (p.u)	0.00067	0.00057	0.00068	0.00059
F	0.896	0.898	0.901	0.619
PAR	1.0045	1.0055	1.0060	1.0048
V_{min}(p.u)	0.9242	0.9246	0.9246	0.9246
Utility Cost (€)	10019.8	10030.1	10102.1	10055.8
Consumer Cost (€)	2212.1	2214.9	2213.8	2214.1

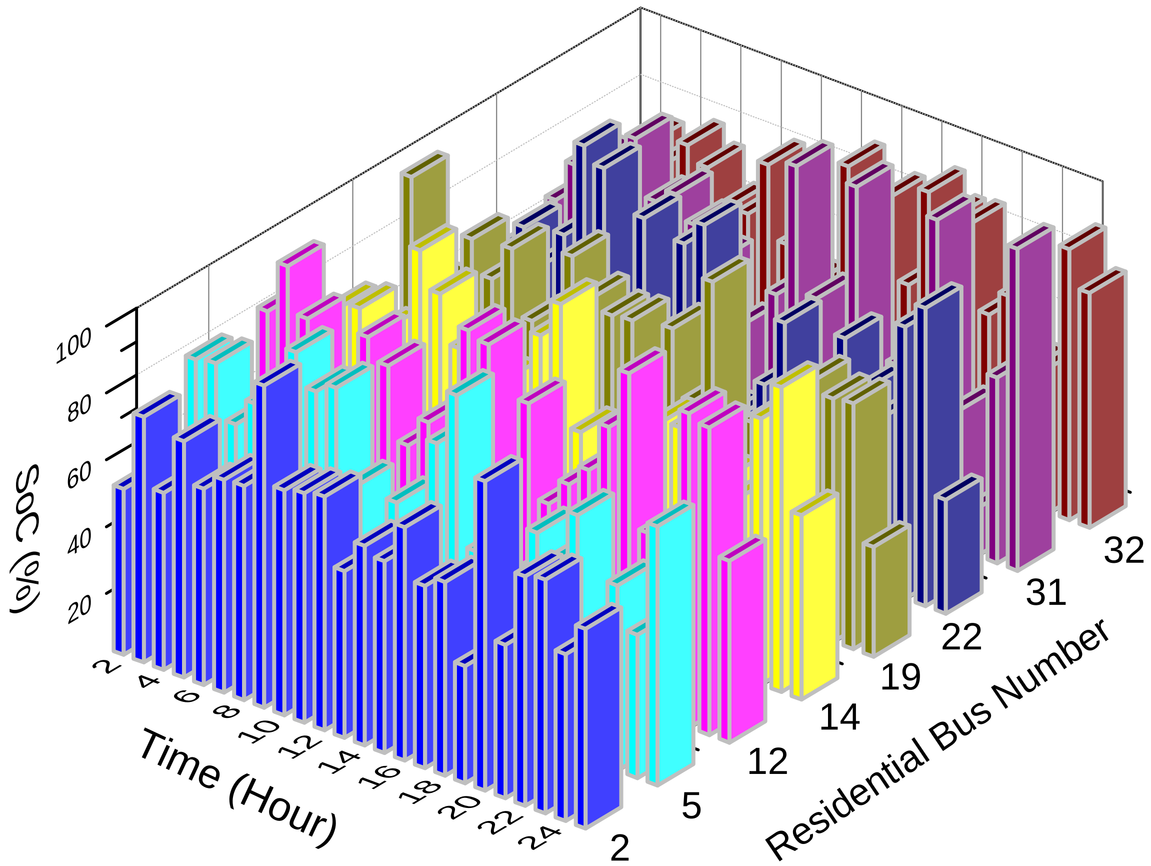

Figure 5.21: Hourly SOC availability at departure time on residential bus

5.6 Summary

In this chapter, a 24-hour day ahead scheduling of PHEVs, D-BESS and DGs to optimize system operating cost, CO_2 emission, energy losses and load flattening was proposed. To segregate the effects of PHEVs, D-BESS and DGs scheduling on distribution system, different case studies are also performed so that one may be able to understand their individual and combined effects. The proposed strategy was implemented on a 38-bus distribution system. It was observed that the energy losses, CO_2 emission, load flatting and voltage profile are significantly improved with the little sacrifice of the utility operating cost of the system.